



# Large area Bragg grating for pump recycling in cladding-pumped multicore erbium-doped fiber amplifiers

CHARLES MATTE-BRETON, LAURIS TALBOT,  YOUNÈS MESSADDEQ, MARTIN BERNIER, AND SOPHIE LAROCHELLE\* 

COPL, Université Laval, Québec G1V 0A6, Canada

\*[sophie.larochelle@gel.ulaval.ca](mailto:sophie.larochelle@gel.ulaval.ca)

**Abstract:** We demonstrate for the first time that a Bragg grating can be written over a large area inside the cladding of a multicore erbium-doped fiber amplifier to increase the power conversion efficiency (PCE) by recycling the output pump power. Our results indicate that a Bragg grating covering ~25% of the cladding area allows us to recycle 19% of the output pump power which leads to a relative increase of the PCE by 16% for an input pump power of 10.6 W in the specific case of an eight-core erbium-doped fiber with a length of 20.3 m and one core loaded with an input signal power of 1.5 dBm.

© 2022 Optica Publishing Group under the terms of the [Optica Open Access Publishing Agreement](#)

## 1. Introduction

Cladding-pumped multicore erbium-doped fiber amplifiers (CP-MC-EDFAs) are a promising technology for cost-reduction in optical communication networks since they simultaneously provide gain to multiple cores, sharing the same cladding, with a single low-cost multimode pump laser diode having a high electrical to optical conversion efficiency. However, one of the main drawbacks for cladding pumping is the lower pump intensity in the doped core, compared to core pumping, due to the total pump power being distributed over the whole cladding area of the fiber. This lower pump intensity results in lower saturation output power that limit gain and bandwidth of CP-MC-EDFAs for C-band amplifiers. Consequently, high pump power must be used to maintain the inversion level of the erbium ions over the whole fiber length which leads to a high amount of unabsorbed output pump power. Therefore, achieving high power conversion efficiency (PCE), from the pump to the signal, can be challenging in cladding-pumped amplifiers in comparison to core-pumped ones.

To mitigate this drawback, higher core density [1], decreased cladding area [2], erbium-ytterbium co-doping [3] and an annular doping geometry [4] have all been proposed. Pump recycling has also been investigated and has been demonstrated in CP-MC-EDFAs by using a side-coupled pump collector [5], cascaded side-coupled pump collectors [6] or turbo cladding pumping with free space optics [7]. All these methods consist in using one or multiple pump collectors at the fiber output, and passive fiber loops, to route the pump power back to the input of the active fiber, recycling as much as 55.2% of the residual pump power [7]. The main drawbacks of these methods are the increased complexity due to the additional components and the corresponding additional input and output signal loss.

Another promising technology for pump recycling is to use inner-cladding Bragg gratings (ICBGs), which are all-fiber reflectors written directly in the cladding of cladding-pumped erbium doped fibers to reflect the pump. ICBGs have been previously used to recycle the unabsorbed pump light of single-core cladding-pumped high-power fiber lasers [8–9]. For example, an ICBG with an effective reflectivity of 58% was inscribed at the end of a 29 W erbium-doped fiber laser emitting at 1.6  $\mu\text{m}$ , which allowed to significantly increase the laser efficiency [10]. This Bragg grating component only reflects light at the pump wavelength while letting through

the laser light propagating inside the fiber core. The ICBGs also have the advantages of being able to handle high power, do not require additional components and leave the fiber tip free of any constraints. Therefore, increasing the PCE with such a component is a promising approach to shorten the required length of active fiber in fiber lasers and decrease the required pump power for amplifier systems. To our knowledge, ICBGs have not yet been investigated in the context of CP-MC-EDFAs that are currently being considered to increase spatial density in optical communication networks [11].

This paper aims to compare the PCE of a CP-MC-EDFA with and without an ICBG. To achieve this goal, in section 2, we first write such a grating covering  $\sim 25\%$  of the cladding area of a double-cladding 8-core fiber with annular doping, which was initially designed for low gain compression [12]. Then, in section 3, the internal gain and noise figure (NF) are measured experimentally with and without an ICBG and the resulting PCE is determined. Finally, in section 4, the experimental results are compared with simulations to estimate the effective percentage of reflected output pump power in the presence of ICBG. We find that the pump effective reflectivity reaches 19%, resulting in a PCE increase of 16%.

## 2. ICBG inscription

In this paper, the CP-MC-EDFA is based on the 8-core fiber extensively described in [12]. Each core, single mode in the C-band and undoped, is surrounded by an annular erbium-doped region located in the cladding. This design mitigates saturation effects since only the low intensity evanescent tail of the guided signal mode interacts with the doped region. Aluminophosphosilicate is used in the doped region of the cladding to reduce the refractive index change while limiting the percentage of paired ions [12]. The pure-silica cladding, surrounded by a low refractive index fluoroacrylate coating, has a NA of 0.46 and a diameter of 140  $\mu\text{m}$  that make it viable for cladding pumping. The cores are placed along a ring with a radius of 2.3  $\mu\text{m}$  and the distance between two cores is 38  $\mu\text{m}$  as shown in Fig. 1. In [12], a MC-CP-EDFA was assembled with this fiber. With a fiber length of 19.8 m and 24.0 W of pump injected in the cladding, the amplifier provided a gain  $> 15.3$  dB and a noise figure  $< 5.4$  dB over the C-band with all the cores loaded with  $1.4 \pm 0.3$  dBm. Under these conditions, it is estimated that 12.8 W of unused pump power exit the fiber at the amplifier output.

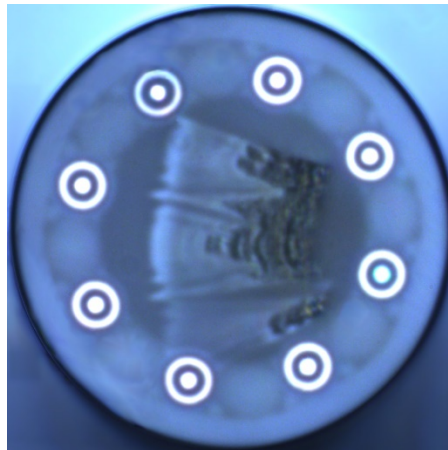


**Fig. 1.** Cross section of the 8-core fiber with an inner-cladding Bragg grating. It was measured with a phase-contrast microscope. The inscription laser beam is incident from the left.

The ICBG was obtained by photo-inscribing a periodic refractive index modulation inside the fiber cladding. As pure silica is not photosensitive to standard UV illumination, we relied on the femtosecond laser inscription [13]. To this end, we used the setup shown in Fig. 1 of Ref. [10], except for the capillary around the fiber that was not present in our case, and employed a Ti-Sapphire regenerative amplifier system (Astrella, Coherent Inc.) that emits 800 nm pulses at a repetition rate of 1 kHz. The laser beam was then frequency doubled to 400 nm [14] using a BBO crystal (EKSMa optics, BBO 1502). The beam, which has a diameter of 11 mm, was afterwards sent through the fiber cladding [14] with an acylindrical lens having a 10 mm focal length. This allowed to reach sufficient light intensity inside the glass to induce a refractive index change by multiphotons absorption [15]. The interference pattern required to inscribe a periodic refractive index modulation was generated thanks to the use of the phase mask-scanning technique [16–17]. An in-house fabricated phase mask, having a central period of 677.5 nm, was placed between the acylindrical lens and the fiber. It created an interference pattern in the spatial region where the diffracted  $\pm 1$  orders of the femtosecond beam overlapped with a period corresponding to half of that of the phase mask. Given the Bragg equation and the fiber's cladding refractive index, it inscribed an ICBG with a reflection peak centered at 981 nm. Such wavelength was chosen given the availability of a wavelength-stabilized laser diode emitting at that wavelength (BWT, model K981AN1RN-90.00W) which was used as the pump source for the CP-MC-EDFA. This wavelength is also close to the 979 nm peak absorption wavelength of the multicore fiber [12]. The phase mask was chosen with a period chirp rate of 1.2 nm/cm across its length. Given the highly multimode propagation of the pump light inside the cladding, a chirped ICBG is needed to cover a range of different effective refractive indices. In the present case, the ICBG covers effective refractive indices from 1.4432 to 1.4527, at the pump wavelength given the chirp rate of the phase mask and the 3.7 cm grating length. This chirp rate was chosen given the availability of this phase mask and because it was shown to optimize the reflectivity of ICBGs in a previous experiment, but with a different fiber-laser system [8]. In the future, optimizing the chirp rate for the specific NA of the fiber cladding and pump injection conditions, as described later, should increase the effective ICBG reflectivity.

Given the non-linear nature of photo-induced index change process in pure silica by fs writing at 400 nm, and the short focal length of the acylindrical lens, refractive index modifications occur only in the close vicinity of the laser beam focus. When focused at the center of the fiber, the beam induces a refractive index modulation over a depth of about 10  $\mu\text{m}$  and a height of about 1  $\mu\text{m}$ . Therefore, in order to increase the transverse area covered by the ICBG, and ultimately its reflectivity, the beam had to be scanned over the fiber cladding cross-section. To this end, the acylindrical lens of the writing setup was placed on a 2D piezoelectric stage allowing to move the focal point of the femtosecond beam. The piezoelectric actuator moving the height of the lens, was driven at a 1 Hz frequency with a peak-to-peak amplitude of 100  $\mu\text{m}$ , while the other actuator moving the focus depth was driven at 0.133 Hz over the same amplitude. These different frequencies were chosen to focus pulses over the largest possible fraction of the fiber transverse area.

To write a grating of a few cm long, we used the phase mask scanning technique that consists in moving both the laser beam and the acylindrical lens along the fiber axis using a motorized translation stage, while the fiber and the phase mask remained still. During the 30-minute inscription process, the beam was scanned over a fiber length of 2.6 cm that was stripped of its coating beforehand. This led to a 3.7 cm long ICBG when taking into account the 11 mm inscription beam diameter. Such a slow longitudinal scanning speed allowed to send multiple pulses at each grating position in the fiber cross-section so as to increase the refractive index modification. We used an average laser power of 190 mW, with a pulsewidth of 40 fs and a repetition rate of 1 kHz. Then, the short fiber segment containing the grating was thermally annealed at 475°C for 10 minutes with an oven as a standard procedure to reduce the photoinduced

absorption losses. Finally, it was recoated with the same low-index polymer that was used during fiber drawing.

The cross-section of an ICBG inscribed in the 8-core fiber under the same conditions as the one tested with the amplifier is shown in Fig. 1. The grating only covers about ~25% of the cladding area, which was determined by manually defining the grating and cladding areas in Fig. 1 and using an image processing software afterwards to count the number of pixels for each region. The area of ~25% limits the maximum achievable ICBG reflectivity and means that the grating has a different effective reflectivity for each mode depending on their spatial overlap. The modes with higher  $n_{\text{eff}}$ , which are mainly confined into the center of the cladding, and thus less absorbed by the doped regions, are also likely to experience a stronger reflectivity. Furthermore, the ICBG cross-section has a conical shape due to the curvature of the fiber cladding. Given the large number of pump cladding modes, which includes both even and odd modes, this grating asymmetry can be helpful to reflect odd modes. As the laser beam is scanned perpendicularly to the fiber axis during the inscription process, the beam is refracted at different angles depending on its instantaneous height on the cladding that introduces a lensing effect. Also, noting that the writing process is a nonlinear phenomenon, regions where the focusing effect are the highest exhibit a stronger refractive index modulation as can be observed on the right of the ICBG in Fig. 1. This effect limits the maximum reachable ICBG area since these hot spots could induce signal losses if they overlapped a core. In the future, it could be circumvented by inserting the fiber inside a hollow capillary with an inner diameter slightly larger than the fiber cladding diameter and a significantly larger outer diameter, that has been shown to improve grating uniformity and increase the scanning area [10] or by using a different beam scanning technique [18], allowing to significantly increase the grating area and reflectivity.

The transmission spectrum of the ICBG is shown in Fig. 2. It was measured by injecting the light of a supercontinuum laser source (Koheras, NKT Photonics) inside a 1 m long fiber segment containing the grating and by using a bare fiber adapter to connect the output to an OSA. The power spectrum was measured before and after the ICBG inscription. It is worth noting that the free space optical input of the OSA has a NA of 0.105, which is significantly lower than the NA of the fiber cladding (0.46). Therefore, the transmittance shown in Fig. 2 only applies to the lower order cladding modes. An insertion loss of -3.7 dB is observed at 981 nm from which we can deduce a maximum peak reflectivity of 57%. The transmittance above 0 dB observed near 950 nm and 1000 nm is due to the noise of the supercontinuum laser source used for this measurement. While no significant losses were measured for wavelengths outside of the Bragg resonance, it is possible that a fraction of this measured insertion loss could also be caused by coupling of the 981 nm light to some radiative modes, which was confirmed by observing the fiber with an infrared viewer.

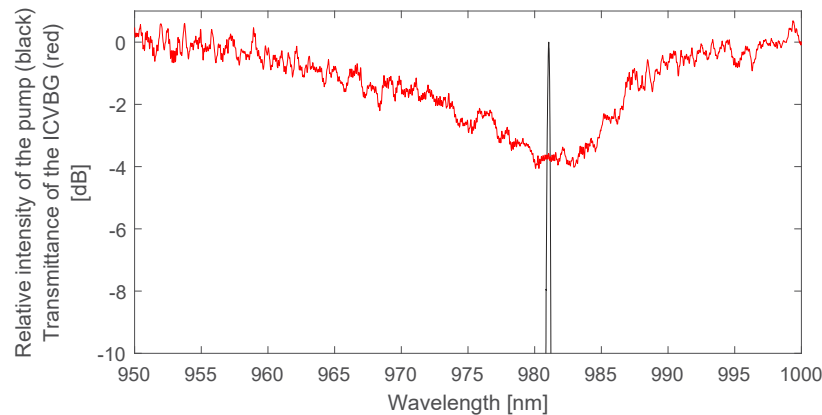


**Fig. 2.** Normalized spectral intensity of the 981-nm wavelength-controlled pump source for an output pump power of 10.0 W (black) and transmission spectrum of an ICBG written with the phase mask used for this investigation (red).

### 3. Gain and NF measurement results

In this section, we aim to determine the internal gain, NF and PCE of the CP-MC-EDFA in two distinct configurations: i) when an ICBG is used to recycle the pump power and ii) when the pump power is not recycled. To determine the internal gain and NF with and without the ICBG, we first did the measurements with an ICBG, for a doped fiber length of 20.3 m, as shown in Fig. 3. Then, we removed the last 0.7 m of doped fiber near the output, between points B and C in Fig. 3, which included the ICBG, and made a new output splice and pump dump to, afterwards, repeat the measurements without the ICBG with a doped fiber length of now 19.6 m.

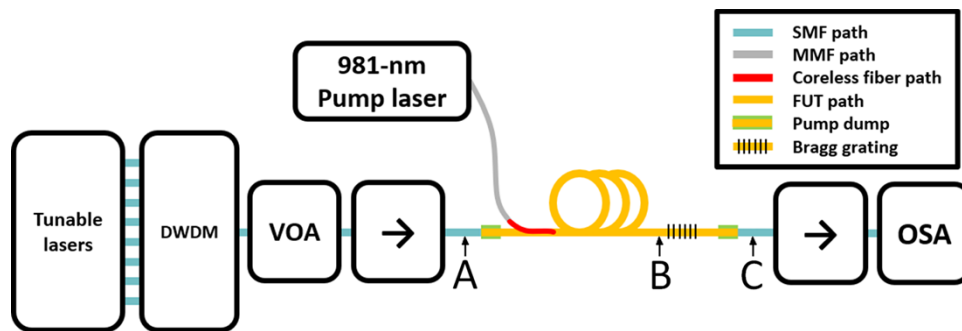


**Fig. 3.** Setup configuration used to measure the gain and NF with and without an ICBG.

The total signal power was uniformly distributed over eight spectral channels generated by eight tunable lasers centered at 1528.8 nm, 1532.7 nm, 1539.2 nm, 1543.7 nm, 1549.3 nm, 1554.9 nm, 1559.8 nm and 1563.9 nm. For these measurements, only one of the cores was loaded with signal power. To identify the same core that was used for the single core characterization reported for this fiber in [12], the absorption at 1530 nm was measured in each of the 8 cores of the fiber under test (FUT). Using the same core was important considering that some of the parameters used in the simulations, namely the concentration of paired ions, could have core-to-core variations and were only measured in this core. Then, using an active alignment system, single-mode fibers (SMFs) were spliced to both ends of the FUT into the selected core and a total loss of 2.4 dB was measured between points A and C in Fig. 3 using a 1300 nm tunable laser. The variable optical

attenuator (VOA) was then adjusted so that the total signal power at the input of the active fiber, when considering 1.2 dB of loss per SMF-FUT splice, was 1.5 dBm. Also, the pump power was coupled into the cladding of the FUT with an unfused half-taper [19] made by splicing a 105/125  $\mu\text{m}$  fiber to a coreless pure-silica fiber that was tapered to obtain a downtaper length of 8.0 cm and a waist length of 2.5 cm. The pump coupling region is located 10 cm after the input splice. The achieved coupling efficiency was  $93\% \pm 1\%$  with the 981 nm wavelength-stabilized pump diode mentioned previously (BWT). To avoid damaging the isolators, cladding pump strippers were made at both ends of the FUT by applying high index polymer over 3 cm at the input and output of the fiber, directly next to the splices. It is also worth noting that the ICBG was located 55 cm before the output splice. The total fiber length for the FUT was 20.3 m. The gain and NF were measured when a current of 0.0 A, 1.3 A, 1.4 A, 1.5 A, 1.6 A, 1.7 A, 1.8 A, 1.9 A and 2.0 A was applied to the pump laser diode. Below, we show that these currents correspond to a coupled pump power of 0 W, 5.2 W, 5.9 W, 6.6 W, 7.4 W, 8.2 W, 9.0 W, 9.7 W and 10.6 W. The spectral gain and noise figure (NF) measurement results are shown in Fig. 4 and 5 (red circles).

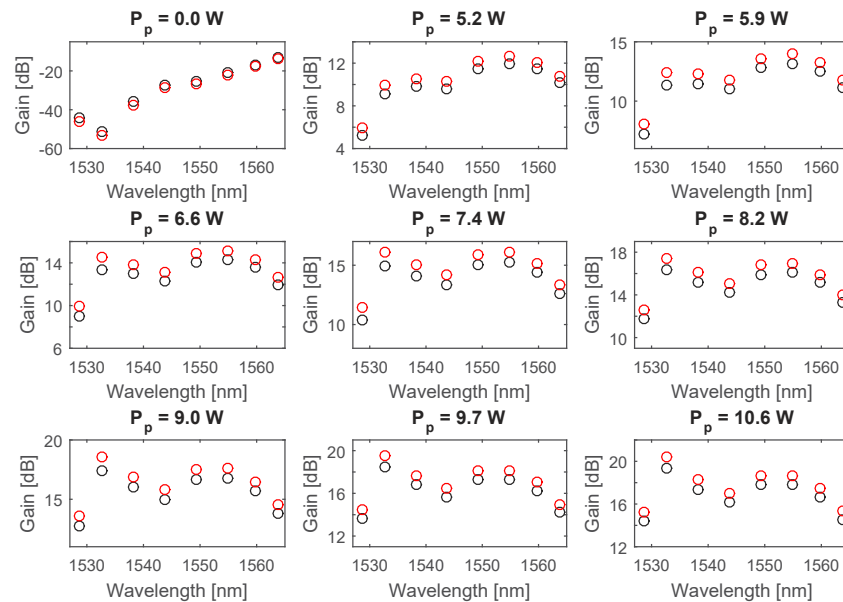


**Fig. 4.** Gain measurement results for a total input signal power of 1.5 dBm, and various input pump power ranging from 0 W to 10.6 W when i) an ICBG is used to recycle the output pump power (red) with a fiber length of 20.3 m and ii) when the pump is not recycled (black) with a fiber length of 19.6 m.

After measuring the gain and NF with the setup configuration of Fig. 3, we cut the FUT 10 cm before the output splice, measured the output pump power with a free-space power meter, then cut the FUT 10 cm before the ICBG, for a new fiber length of 19.6 m and measured the output pump power again. The results, shown in Fig. 6, indicate that the transmittance of the ICBG at the pump wavelength is 40% on average, which is good agreement with the 3.7 dB observed at 981 nm in Fig. 2. We then made a new splice using an active alignment and the same splice recipe as previously, as well as a new pump dump right before the splice. To ensure a proper comparison, the input splice, VOA, and half-taper pump coupler were left untouched. The insertion loss at 1300 nm was measured again and, was also 2.4 dB for this configuration, indicating that the ICBG did not cause any significant degradation of the core signal. The gain



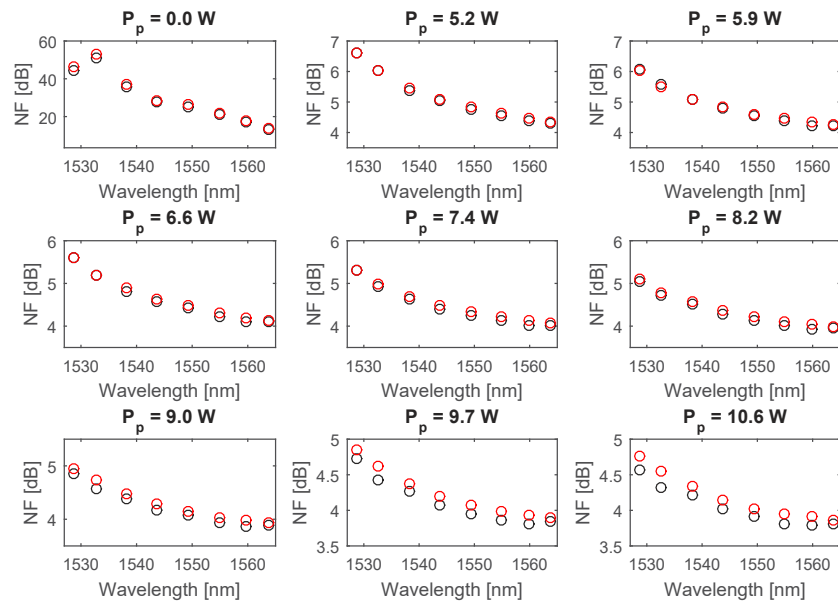


**Fig. 5.** NF measurement results for a total input signal power of 1.5 dBm, and various input pump power ranging from 0 W to 10.6 W when i) an ICBG is used to recycle the output pump power (red) with a fiber length of 20.3 m and ii) when the pump is not recycled (black) with a fiber length of 19.6 m.

and NF were then measured again for the same pump laser diode current setpoints. The results are also shown in Fig. 4 and 5 (black circles).

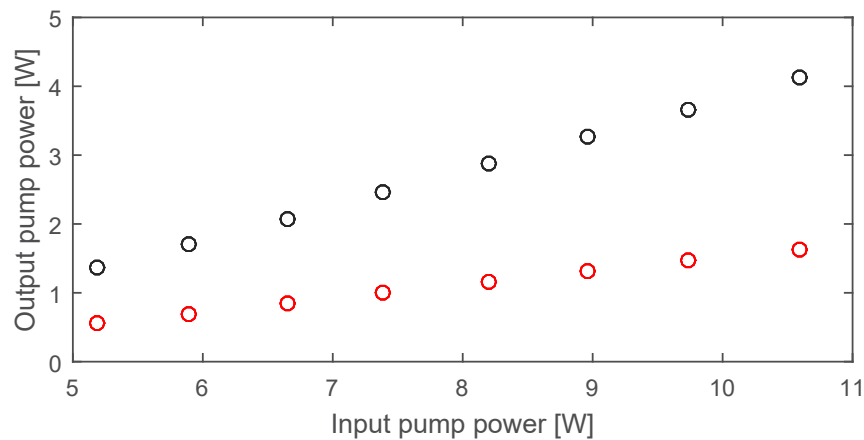


**Fig. 6.** Measurement results for the output pump power as a function of the input pump power (without an input signal) for a fiber length of 19.6 m without ICBG (black) and a fiber length of 20.2 m with an ICBG (red).

When all gain and NF measurements were completed, the FUT was cut 1.0 m after the pump coupler and we measured the exiting pump power with a free-space power meter. The input pump power was then estimated from these results, by multiplying the measured pump power by 1.012 to account for the pump background loss of  $0.012 \text{ m}^{-1}$  or  $0.052 \text{ dB/m}$  over 1.0 m of fiber

length. This measurement allowed us to determine that the pump laser diode current setpoints used for the gain and NF measurements correspond to coupled pump power of 0 W, 5.2 W, 5.9 W, 6.6 W, 7.4 W, 8.2 W, 9.0 W, 9.7 W and 10.6 W.

Finally, the measured coupled pump power, input signal power and gain were used to calculate the PCE with and without an ICBG. The resulting PCE as a function of input pump power is shown in Fig. 7. Such low PCE can be explained by the fact that only one core was used, and the fiber length was not optimized. Nevertheless, the PCE is 23% higher in the configuration for which an ICBG was used compared to the configuration for which the pump was not recycled, when the input pump power was set to 10.6 W. It is however worth noting that a longer fiber length of 20.3 m, instead of 19.6 m, was used in the configuration with the ICBG. This aspect will be discussed in more details in the next section.

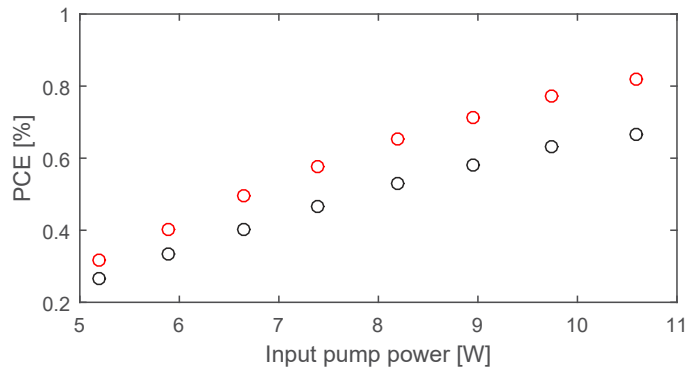


**Fig. 7.** PCE as a function of input pump power for an input signal power of 1.5 dBm when an ICBG is used to recycle the output pump power with a fiber length of 20.3 m (red) and when the pump is not recycled with a fiber length of 19.6 m (black).

#### 4. Simulation results and discussion

In this section, we first estimate the effective reflectivity of the ICBG by fitting spectral gain and NF simulations to the measurement results. We then determine the relative increase of the PCE caused by the ICBG for a fixed fiber length.

For the simulations, we first used the model and parameters determined in [12], namely, a pump background loss of  $0.012 \text{ m}^{-1}$ , a paired ions concentration of 7% and a pump absorption cross-section of  $2.2 \times 10^{-25} \text{ m}^2$  at 981 nm (for the latter see Fig. 7 of [12]). To have a better spectral resolution in the simulations, we consider 37 signal channels between 1528 nm and 1564 nm, for a resolution of 1 nm, and a total input signal power of 1.5 dBm. For the spectral gain, a good agreement was obtained between the simulation results and the experimental measurements without an ICBG with a root mean square error (RMSE) of 0.6 dB.

We then modified the model to also consider a contra-propagating pump power, uniformly distributed over the cladding, with an initial power equal to the output pump power of the co-propagating pump power times an effective reflectivity  $R$ . In the simulations, we assumed the pump power to be coupled into the fiber at the longitudinal position  $z = 0 \text{ m}$  and to be reflected by the ICBG at the output of the active fiber,  $z = 20.3 \text{ m}$ .

Then, to estimate the effective reflectivity  $R$  of the ICBG, we computed the RMSE between the 72 data points of the measured gain with or without the ICBG (shown in Fig. 4) and the corresponding simulated gain results for given values of  $R$ . The RMSE is plotted as a function of the effective reflectivity in Fig. 8. As expected, when there is no ICBG and the fiber length is set to 19.6 m (black), the fit is optimal for an effective reflectivity of 0%. When an ICBG is present



in the fiber cladding for pump recycling and considering a fiber length of 20.3 m (red), the fit is optimal for an effective reflectivity of 19%.

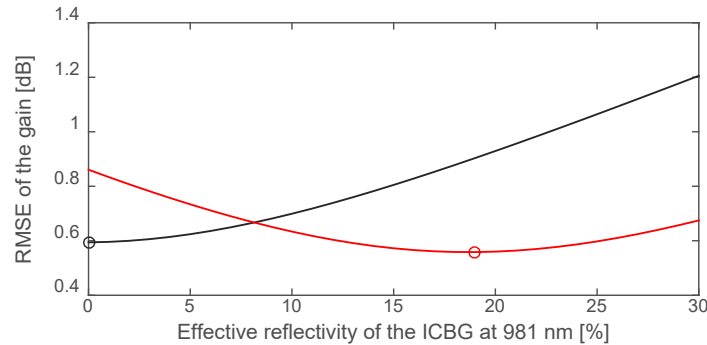


**Fig. 8.** RMSE between the simulated and measured gain as a function of the ICBG effective reflectivity when an ICBG is used to recycle the output pump power and considering a fiber length of 20.3 m (red). For comparison, the RMSE between the simulated and measured gain is also shown when there is no ICBG and considering a fiber length of 19.6 m (black). The circles indicate the optimal fit.

In Fig. 9 and 10, the simulation results obtained when using the previously determined effective reflectivity (0% when the pump is not recycled and 19% when the ICBG is used for pump recycling) are compared with the gain and NF measurements for the various pump powers reported in section 3.

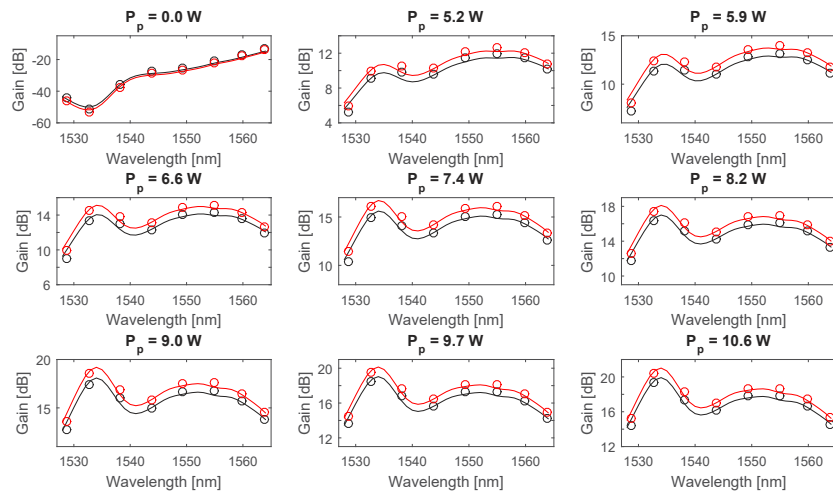


**Fig. 9.** Gain measurement (circles) and simulations (lines) for a total input signal power of 1.5 dBm, and various input pump power ranging from 0 W to 10.6 W, when i) an ICBG is used to recycle the output pump power (red) with a fiber length of 20.3 m and assuming  $R = 19\%$  for the simulations; and ii) when the pump is not recycled (black) with a fiber length of 19.6 m and assuming  $R = 0\%$  for the simulations.

The experimental results shown in Fig. 7 indicate a 23% increase in the PCE when  $P_p = 10.6$  W. These results were however obtained with slightly different conditions for the fiber length. According to our simulations and using the fiber parameters described above, when no ICBG is used, for input signal power of 1.5 dBm and input pump power of 10.6 W, increasing the

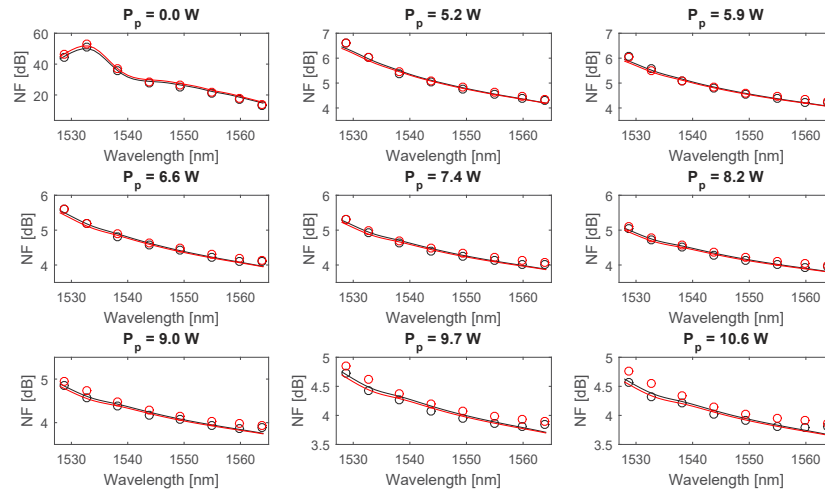


**Fig. 10.** NF measurement (circles) and simulations (lines) for a total input signal power of 1.5 dBm, and various input pump power ranging from 0 W to 10.6 W, when i) an ICBG is used to recycle the output pump power (red) with a fiber length of 20.3 m and assuming  $R = 19\%$  for the simulations; and ii) when the pump is not recycled (black) with a fiber length of 19.6 m and assuming  $R = 0\%$  for the simulations.

fiber length from 19.6 m to 20.3 m increases the PCE by 6%. Thus, the actual PCE increase that is caused by the recycled pump, and not the fiber length, is actually  $(1.23/1.06 - 1) = 16\%$ . An increase of 16% for the PCE when only recycling 19% of the output pump power, which corresponds to 19% of  $\sim 780$  mW, can be explained by the fact that the last meters of the fiber have a lower average inversion level. Therefore, increasing the pump power over this part of the active fiber has a more significant positive impact on the performance than recycling the pump power by reinjecting it at the input of the fiber.

Considering the same 981 nm pump wavelength and coupled pump power of 10.6 W, we now use simulations to estimate the PCE that would be obtained if the input signal power was set to 1.5 dBm per core in all eight cores and if the fiber length was adjusted to maximize the PCE for various values of effective reflectivity  $R$ , between 0% and 100%. The results are shown in Fig. 11 and indicate that an ideal ICBG could theoretically lead to an increase of the PCE by 52%, from 7.9% to 12.0%. Also, the optimal fiber length was 30.8 m for  $R = 0\%$  and 27.3 m for  $R = 100\%$ , indicating that pump recycling also allows decreasing the required fiber length. Lastly, we note that the 8-core fiber with annular doping used in this study was designed to achieve low gain compression in multi-core amplifiers designed for dynamic network. Considering that more pump power would be reflected under the low input signal power conditions, compared to high input signal power conditions, recycling the pump may not be beneficial to the gain compression performance. Nonetheless, the results clearly show the benefits in terms of PCE that are obtained by the introduction of ICBG for pump recycling and this technique could easily be implemented to more standard CP-MC-EDFA designs with uniform doping in the core.

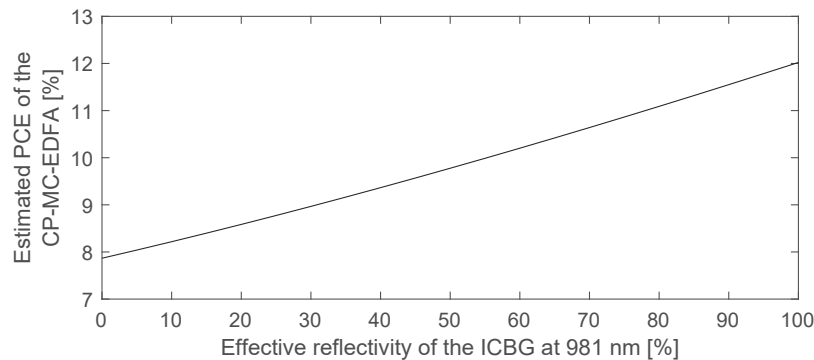


**Fig. 11.** Calculated PCE for a fully loaded CP-MC-EDFA as a function of the effective reflectivity of the ICBG at 981 nm. The 8 cores are loaded with an input signal power of 1.5 dBm per core, the pump wavelength is 981 nm, the coupled pump power is 10.6 W and the fiber length is adjusted for each value of  $R$  to maximize the PCE.

## 5. Conclusion

In summary, we were able to demonstrate, for the first time of our knowledge, pump recycling with a Bragg grating inscribed in the cladding of a CP-MC-EDFA. The technique uses readily available Bragg grating writing technology and presents a low complexity solution to implement pump recycling. According to our simulations, the effective reflectivity of the ICBG was 19%, which led to a relative increase of 16% for the PCE. These results are very promising considering that significant pump power is typically lost at the output of CP-EDFAs given that high pump intensity is required for the signal to be properly amplified. In this paper, although we achieved a pump recycling ratio of only 19%, compared to the record of 55.2% achieved with turbo cladding pumping [7], the proposed method has the advantage of not requiring any additional component and, therefore, has the potential of becoming a scalable and economically viable solution for pump recycling provided that techniques to decrease the inscription time and to increase the ICBG efficiency can be developed. Currently only ~25% of the cladding area covered by the ICBG and, therefore, improvement in the grating effective reflectivity is expected as the writing technique is refined to increase the grating area and uniformity. Considering the high electrical to optical conversion efficiency of low-cost multimode laser diode used with cladding pumping, using ICBGs for pump recycling might be the very last step required to make cladding pumping more economically viable than core pumping in communication networks.

**Funding.** Natural Sciences and Engineering Research Council of Canada.

**Disclosures.** The authors declare no conflicts of interest.

**Data availability.** Data underlying the results presented in this paper are not publicly available at this time but may be obtained from the authors upon reasonable request.

## References

1. S. Takasaka, K. Maeda, K. Kawasaki, K. Yoshioka, H. Oshio, R. Sugizaki, Y. Kawaguchi, H. Takahashi, and M. Shiino, "Increase of cladding pump power efficiency by a 19-core erbium doped fibre amplifier," in *Proc. Eur. Conf. Opt. Commun.*, 2017, Paper Th.2.D.
2. C. Jin, B. Huang, K. Shang, H. Chen, R. Ryf, R. J. Essiambre, N. K. Fontaine, G. Li, L. Wang, Y. Messaddeq, and S. LaRochelle, "Efficient annular cladding amplifier with six, three-mode cores," in *Proc. Eur. Conf. Opt. Commun.*, 2015, Paper PDP.2.1.
3. G. Mélin, R. Kerampran, A. Monteville, S. Bordais, T. Robin, D. Landais, A. Lebreton, Y. Jaouën, and T. Taunay, "Power efficient all-fiberized 12-core erbium/ytterbium doped optical amplifier," in *Proc. Opt. Fiber Commun. Conf.*, 2020, Paper M.4.C.2.

4. C. Matte-Breton, H. Chen, N. K. Fontaine, R. Ryf, R.-J. Essiambre, C. Kelly, C. Jin, Y. Messaddeq, and S. LaRochelle, "Demonstration of an erbium-doped fiber with annular doping for low gain compression in cladding-pumped amplifiers," *Opt. Express* **26**(20), 26633–26645 (2018).
5. S. Takasaka, K. Maeda, K. Kawasaki, K. Yoshioka, R. Sugizaki, and M. Tsukamoto, "Cladding Pump Recycling Device for 19-core EDFA," in *Proc. Opt. Fiber Commun. Conf.*, 2019, Paper Th.3.D.7.
6. K. Maeda, S. Takasaka, K. Kawasaki, K. Yoshioka, R. Sugizaki, and M. Tsukamoto, "Cladding pump recycling using cascaded pump collectors in 7-core EDFA," in *Proc. Eur. Conf. Opt. Commun.*, 2019, Paper P.12.
7. H. Takeshita, K. Matsumoto, S. Yanagimachi, and E. L. T. de Gabory, "Configurations of pump injection and reinjection for improved amplification efficiency of turbo cladding pumped MC-EDFA," *J. Lightw. Technol.* **38**(11), 2922–2929 (2020).
8. L. Talbot, P. Paradis, and M. Bernier, "All-fiber laser pump reflector based on a femtosecond-written inner cladding Bragg grating," *Opt. Lett.* **44**(20), 5033–5036 (2019).
9. S. Baek, D. B. S. Soh, Y. Jeong, J. K. Sahu, J. Nilsson, and B. Lee, "A cladding-pumped fiber laser with pump-reflecting inner-cladding Bragg grating," *IEEE Photonics Technol. Lett.* **16**(2), 407–409 (2004).
10. L. Talbot, L. C. Michaud, V. Boulanger, P. Paradis, and M. Bernier, "Inner-cladding pump reflector based on chirped volume Bragg gratings," *Proc. SPIE* **11261**, 26 (2020).
11. K. S. Abedin, J. M. Fini, T. F. Thierry, V. R. Supradeepa, B. Zhu, M. F. Yan, L. Bansal, E. M. Monberg, and D. J. DiGiovanni, "Multicore erbium doped fiber amplifiers for space division multiplexing systems," *J. Lightwave Technol.* **32**(16), 2800–2808 (2014).
12. C. Matte-Breton, R.-J. Essiambre, C. Kelly, Y. Messaddeq, and S. LaRochelle, "Multicore Cladding-Pumped Fiber Amplifier with Annular Erbium Doping for Low Gain Compression," *J. Lightwave Technol.* **40**(6), 1836–1846 (2022).
13. S. J. Mihailov, C. W. Smelser, D. Grobnic, R. B. Walker, P. Lu, H. Ding, and J. Unruh, "Bragg gratings written in all-SiO<sub>2</sub> and Ge-doped core fibers with 800-nm femtosecond radiation and a phase mask," *J. Lightwave Technol.* **22**(1), 94–100 (2004).
14. M. Bernier, R. Vallée, B. Morasse, C. Desrosiers, A. Saliminia, and Y. Sheng, "Ytterbium fiber laser based on first-order fiber Bragg gratings written with 400 nm femtosecond pulses and a phase-mask," *Opt. Express* **17**(21), 18887–18893 (2009).
15. K. M. Davis, K. Miura, N. Sugimoto, and K. Hirao, "Writing waveguides in glass with a femtosecond laser," *Opt. Lett.* **21**(21), 1729–1731 (1996).
16. J. Thomas, E. Wikszak, T. Clausnitzer, U. Fuchs, U. Zeitner, S. Nolte, and A. Tünnermann, "Inscription of fiber Bragg gratings with femtosecond pulses using a phase mask scanning technique," *Appl. Phys. A* **86**(2), 153–157 (2006).
17. S. J. Mihailov, D. Grobnic, C. W. Smelser, P. Lu, R. B. Walker, and H. Ding, "Bragg grating inscription in various optical fibers with femtosecond infrared lasers and a phase mask," *Opt. Mater. Express* **1**(4), 754–765 (2011).
18. L. Talbot, S. Pelletier-Ouellet, F. Trépanier, and M. Bernier, "Wavelength stabilization of high-power laser diodes using Bragg gratings inscribed in their highly multimode fiber pigtails," *Opt. Lett.* **47**(3), 633–636 (2022).
19. C. Matte-Breton, R. Wang, Y. Messaddeq, and S. LaRochelle, "Novel Fuseless Optical Fiber Side-Coupler based on Half-Taper for Cladding Pumped EDFAs," in *Proc. Opt. Fiber Commun. Conf.*, 2020, Paper T.3.A.2.